EUROPEAN LABORATORY FOR PARTICLE PHYSICS

CERN-PPE/97-168
19 December, 1997

Search for charged Higgs bosons in e^+e^- collisions at $\sqrt{s} = 130 - 172$ GeV

The OPAL Collaboration

Abstract

A search is described to detect charged Higgs bosons via the process $e^+e^- \to H^+H^-$, using data collected by the OPAL detector at center-of-mass energies of 130−172 GeV with a total integrated luminosity of 25 pb^{-1}. The decay channels are assumed to be $H^+ \to q\overline{q}'$ and $H^+ \to \tau^+\nu_\tau$. No evidence for charged Higgs boson production is observed. The lower limit for its mass is determined to be 52 GeV at 95% confidence level, independent of the $H^+ \to \tau^+\nu_\tau$ branching ratio.

(Submitted to Physics Letters B)

The OPAL Collaboration

K. Ackerstaff[8], G. Alexander[23], J. Allison[16], N. Altekamp[5], K.J. Anderson[9], S. Anderson[12], S. Arcelli[2], S. Asai[24], S.F. Ashby[1], D. Axen[29], G. Azuelos[18,a], A.H. Ball[17], E. Barberio[8], R.J. Barlow[16], R. Bartoldus[3], J.R. Batley[5], S. Baumann[3], J. Bechtluft[14], T. Behnke[8], K.W. Bell[20], G. Bella[23], S. Bentvelsen[8], S. Bethke[14], S. Betts[15], O. Biebel[14], A. Biguzzi[5], S.D. Bird[16], V. Blobel[27], I.J. Bloodworth[1], M. Bobinski[10], P. Bock[11], D. Bonacorsi[2], M. Boutemeur[34], S. Braibant[8], L. Brigliadori[2], R.M. Brown[20], H.J. Burckhart[8], C. Burgard[8], R. Bürgin[10], P. Capiluppi[2], R.K. Carnegie[6], A.A. Carter[13], J.R. Carter[5], C.Y. Chang[17], D.G. Charlton[1,b], D. Chrisman[4], P.E.L. Clarke[15], I. Cohen[23], J.E. Conboy[15], O.C. Cooke[8], C. Couyoumtzelis[13], R.L. Coxe[9], M. Cuffiani[2], S. Dado[22], C. Dallapiccola[17], G.M. Dallavalle[2], R. Davis[30], S. De Jong[12], L.A. del Pozo[4], A. de Roeck[8], K. Desch[3], B. Dienes[33,d], M.S. Dixit[7], M. Doucet[18], E. Duchovni[26], G. Duckeck[34], I.P. Duerdoth[16], D. Eatough[16], P.G. Estabrooks[6], E. Etzion[23], H.G. Evans[9], M. Evans[13], F. Fabbri[2], A. Fanfani[2], M. Fanti[2], A.A. Faust[30], L. Feld[8], F. Fiedler[27], M. Fierro[2], H.M. Fischer[3], I. Fleck[8], R. Folman[26], D.G. Fong[17], M. Foucher[17], A. Fürtjes[8], D.I. Futyan[16], P. Gagnon[7], J.W. Gary[4], J. Gascon[18], S.M. Gascon-Shotkin[17], N.I. Geddes[20], C. Geich-Gimbel[3], T. Geralis[20], G. Giacomelli[2], P. Giacomelli[4], R. Giacomelli[2], V. Gibson[5], W.R. Gibson[13], D.M. Gingrich[30,a], D. Glenzinski[9], J. Goldberg[22], M.J. Goodrick[5], W. Gorn[4], C. Grandi[2], E. Gross[26], J. Grunhaus[23], M. Gruwé[27], C. Hajdu[32], G.G. Hanson[12], M. Hansroul[8], M. Hapke[13], C.K. Hargrove[7], P.A. Hart[9], C. Hartmann[3], M. Hauschild[8], C.M. Hawkes[5], R. Hawkings[27], R.J. Hemingway[6], M. Herndon[17], G. Herten[10], R.D. Heuer[8], M.D. Hildreth[8], J.C. Hill[5], S.J. Hillier[1], P.R. Hobson[25], A. Hocker[9], R.J. Homer[1], A.K. Honma[28,a], D. Horváth[32,c], K.R. Hossain[30], R. Howard[29], P. Hüntemeyer[27], D.E. Hutchcroft[5], P. Igo-Kemenes[11], D.C. Imrie[25], K. Ishii[24], A. Jawahery[17], P.W. Jeffreys[20], H. Jeremie[18], M. Jimack[1], A. Joly[18], C.R. Jones[5], M. Jones[6], U. Jost[11], P. Jovanovic[1], T.R. Junk[8], J. Kanzaki[24], D. Karlen[6], V. Kartvelishvili[16], K. Kawagoe[24], T. Kawamoto[24], P.I. Kayal[30], R.K. Keeler[28], R.G. Kellogg[17], B.W. Kennedy[20], J. Kirk[29], A. Klier[26], S. Kluth[8], T. Kobayashi[24], M. Kobel[10], D.S. Koetke[6], T.P. Kokott[3], M. Kolrep[10], S. Komamiya[24], R.V. Kowalewski[28], T. Kress[11], P. Krieger[6], J. von Krogh[11], P. Kyberd[13], G.D. Lafferty[16], R. Lahmann[17], W.P. Lai[19], D. Lanske[14], J. Lauber[15], S.R. Lautenschlager[31], I. Lawson[28], J.G. Layter[4], D. Lazic[22], A.M. Lee[31], E. Lefebvre[18], D. Lellouch[26], J. Letts[12], L. Levinson[26], B. List[8], S.L. Lloyd[13], F.K. Loebinger[16], G.D. Long[28], M.J. Losty[7], J. Ludwig[10], D. Lui[12], A. Macchiolo[2], A. Macpherson[30], M. Mannelli[8], S. Marcellini[2], C. Markopoulos[13], C. Markus[3], A.J. Martin[13], J.P. Martin[18], G. Martinez[17], T. Mashimo[24], P. Mättig[26], W.J. McDonald[30], J. McKenna[29], E.A. Mckigney[15], T.J. McMahon[1], R.A. McPherson[28], F. Meijers[8], S. Menke[3], F.S. Merritt[9], H. Mes[7], J. Meyer[27], A. Michelini[2], S. Mihara[24], G. Mikenberg[26], D.J. Miller[15], A. Mincer[22,e], R. Mir[26], W. Mohr[10], A. Montanari[2], T. Mori[24], S. Mihara[24], K. Nagai[26], I. Nakamura[24], H.A. Neal[12], B. Nellen[3], R. Nisius[8], S.W. O'Neale[1], F.G. Oakham[7], F. Odorici[2], H.O. Ogren[12], A. Oh[27], N.J. Oldershaw[16], M.J. Oreglia[9], S. Orito[24], J. Pálinkás[33,d], G. Pásztor[32], J.R. Pater[16], G.N. Patrick[20], J. Patt[10], R. Perez-Ochoa[8], S. Petzold[27], P. Pfeifenschneider[14], J.E. Pilcher[9], J. Pinfold[30], D.E. Plane[8], P. Poffenberger[28], B. Poli[2], A. Posthaus[3], C. Rembser[8], S. Robertson[28], S.A. Robins[22], N. Rodning[30], J.M. Roney[28], A. Rooke[15], A.M. Rossi[2], P. Routenburg[30], Y. Rozen[22], K. Runge[10], O. Runolfsson[8],

U. Ruppel[14], D.R. Rust[12], K. Sachs[10], T. Saeki[24], O. Sahr[34], W.M. Sang[25], E.K.G. Sarkisyan[23], C. Sbarra[29], A.D. Schaile[34], O. Schaile[34], F. Scharf[3], P. Scharff-Hansen[8], J. Schieck[11], P. Schleper[11], B. Schmitt[8], S. Schmitt[11], A. Schöning[8], M. Schröder[8], M. Schumacher[3], C. Schwick[8], W.G. Scott[20], T.G. Shears[8], B.C. Shen[4], C.H. Shepherd-Themistocleous[8], P. Sherwood[15], G.P. Siroli[2], A. Sittler[27], A. Skillman[15], A. Skuja[17], A.M. Smith[8], G.A. Snow[17], R. Sobie[28], S. Söldner-Rembold[10], R.W. Springer[30], M. Sproston[20], K. Stephens[16], J. Steuerer[27], B. Stockhausen[3], K. Stoll[10], D. Strom[19], R. Ströhmer[34], P. Szymanski[20], R. Tafirout[18], S.D. Talbot[1], P. Taras[18], S. Tarem[22], R. Teuscher[8], M. Thiergen[10], M.A. Thomson[8], E. von Törne[3], E. Torrence[8], S. Towers[6], I. Trigger[18], Z. Trócsányi[33], E. Tsur[23], A.S. Turcot[9], M.F. Turner-Watson[8], I. Ueda[24], P. Utzat[11], R. Van Kooten[12], P. Vannerem[10], M. Verzocchi[10], P. Vikas[18], E.H. Vokurka[16], H. Voss[3], F. Wäckerle[10], A. Wagner[27], C.P. Ward[5], D.R. Ward[5], P.M. Watkins[1], A.T. Watson[1], N.K. Watson[1], P.S. Wells[8], N. Wermes[3], J.S. White[28], G.W. Wilson[27], J.A. Wilson[1], T.R. Wyatt[16], S. Yamashita[24], G. Yekutieli[26], V. Zacek[18], D. Zer-Zion[8]

[1]School of Physics and Astronomy, University of Birmingham, Birmingham B15 2TT, UK
[2]Dipartimento di Fisica dell' Università di Bologna and INFN, I-40126 Bologna, Italy
[3]Physikalisches Institut, Universität Bonn, D-53115 Bonn, Germany
[4]Department of Physics, University of California, Riverside CA 92521, USA
[5]Cavendish Laboratory, Cambridge CB3 0HE, UK
[6]Ottawa-Carleton Institute for Physics, Department of Physics, Carleton University, Ottawa, Ontario K1S 5B6, Canada
[7]Centre for Research in Particle Physics, Carleton University, Ottawa, Ontario K1S 5B6, Canada
[8]CERN, European Organisation for Particle Physics, CH-1211 Geneva 23, Switzerland
[9]Enrico Fermi Institute and Department of Physics, University of Chicago, Chicago IL 60637, USA
[10]Fakultät für Physik, Albert Ludwigs Universität, D-79104 Freiburg, Germany
[11]Physikalisches Institut, Universität Heidelberg, D-69120 Heidelberg, Germany
[12]Indiana University, Department of Physics, Swain Hall West 117, Bloomington IN 47405, USA
[13]Queen Mary and Westfield College, University of London, London E1 4NS, UK
[14]Technische Hochschule Aachen, III Physikalisches Institut, Sommerfeldstrasse 26-28, D-52056 Aachen, Germany
[15]University College London, London WC1E 6BT, UK
[16]Department of Physics, Schuster Laboratory, The University, Manchester M13 9PL, UK
[17]Department of Physics, University of Maryland, College Park, MD 20742, USA
[18]Laboratoire de Physique Nucléaire, Université de Montréal, Montréal, Quebec H3C 3J7, Canada
[19]University of Oregon, Department of Physics, Eugene OR 97403, USA
[20]Rutherford Appleton Laboratory, Chilton, Didcot, Oxfordshire OX11 0QX, UK
[22]Department of Physics, Technion-Israel Institute of Technology, Haifa 32000, Israel
[23]Department of Physics and Astronomy, Tel Aviv University, Tel Aviv 69978, Israel

[24]International Centre for Elementary Particle Physics and Department of Physics, University of Tokyo, Tokyo 113, and Kobe University, Kobe 657, Japan
[25]Institute of Physical and Environmental Sciences, Brunel University, Uxbridge, Middlesex UB8 3PH, UK
[26]Particle Physics Department, Weizmann Institute of Science, Rehovot 76100, Israel
[27]Universität Hamburg/DESY, II Institut für Experimental Physik, Notkestrasse 85, D-22607 Hamburg, Germany
[28]University of Victoria, Department of Physics, P O Box 3055, Victoria BC V8W 3P6, Canada
[29]University of British Columbia, Department of Physics, Vancouver BC V6T 1Z1, Canada
[30]University of Alberta, Department of Physics, Edmonton AB T6G 2J1, Canada
[31]Duke University, Dept of Physics, Durham, NC 27708-0305, USA
[32]Research Institute for Particle and Nuclear Physics, H-1525 Budapest, P O Box 49, Hungary
[33]Institute of Nuclear Research, H-4001 Debrecen, P O Box 51, Hungary
[34]Ludwigs-Maximilians-Universität München, Sektion Physik, Am Coulombwall 1, D-85748 Garching, Germany

[a] and at TRIUMF, Vancouver, Canada V6T 2A3
[b] and Royal Society University Research Fellow
[c] and Institute of Nuclear Research, Debrecen, Hungary
[d] and Department of Experimental Physics, Lajos Kossuth University, Debrecen, Hungary
[e] and Department of Physics, New York University, NY 1003, USA

1 Introduction

The interactions between elementary particles are well described by the Standard Model (SM) [1] which assumes that particle masses are created via the Higgs mechanism [2] through spontaneous symmetry breaking. The Standard Model contains one doublet of complex scalar fields and predicts a single neutral Higgs boson. The minimal extension of the Higgs sector in the Standard Model consists of two Higgs field doublets [3] and predicts five Higgs bosons of which three are neutral (h^0, H^0 and A^0) and two are charged (H^+ and H^-). Despite a wide experimental effort, no evidence for Higgs bosons has yet been observed.

The discovery of a charged Higgs boson would be a clear indication of physics beyond the Standard Model. Supersymmetry [4] is one of the possible extensions of the Standard Model. The Minimal Supersymmetric Extension of the Standard Model (MSSM), is the most popular example of such a model and contains two Higgs field doublets. At tree level it predicts that the charged Higgs boson is heavier than the $W^{\pm}$ boson, ${M_{H^{\pm}}}^2 = {M_{W^{\pm}}}^2 + {M_{A^0}}^2$. Radiative corrections change this prediction [5], however the detection of a charged Higgs boson lighter than the $W^{\pm}$ boson would severely limit the parameter space of the MSSM.

Searches for charged Higgs bosons were carried out at $\sqrt{s} \approx 91$ GeV [6], with the limit $M_{H^{\pm}} > 44.1$ GeV being the most restrictive. In 1995−96 the center-of-mass energy of the LEP collider has been increased in several steps up to 172 GeV. New lower bounds on the mass of the charged Higgs boson above 50 GeV were recently reported [7] by the ALEPH and the DELPHI Collaborations.

On the basis of a study of the reaction $b \to s\gamma$, the CLEO Collaboration [8] has set an indirect lower limit of $M_{H^{\pm}} > (244 + 63/(\tan\beta)^{1.3})$ GeV, where $\tan\beta$ is the ratio of the vacuum expectation values of the two Higgs fields. This limit is valid in the two-doublet extensions of the Standard Model referred as Model II, if the only new particles are the Higgs bosons. However, in supersymmetric models, possible cancellations between contributions of the charged Higgs boson and supersymmetric particles invalidate this limit [9].

The CDF Collaboration recently reported a search for the decay $t \to bH^+$ followed by $H^+ \to \tau^+\nu_\tau$. A lower limit of $M_{H^{\pm}} > 147 - 158$ GeV is derived for very large $\tan\beta$ depending on the $t\bar{t}$ production cross-section. For $\tan\beta < 40$ no limit is derived, since in this regime the assumed decay chain is no longer dominant [10].

Charged Higgs bosons can be produced in pairs in the process $e^+e^- \to H^+H^-$ with a cross-section which to leading order depends only on the Higgs boson mass and the center-of-mass energy [11]. The PYTHIA program [12] is used to calculate the charged Higgs pair-production cross-section, including initial state radiation, at the various e^+e^- collision energies and for various $H^{\pm}$ masses. Higgs bosons decay predominantly to the heaviest fermions kinematically allowed, which in the case of charged Higgs bosons can be $\tau^+\nu_\tau$ or $c\bar{s}$ pairs, since the $c\bar{b}$ decay mode is largely suppressed by the small CKM-matrix element, V_{cb}.

The branching ratio is model-dependent. When combining the results from the various search channels $BR(H^+ \to \tau^+\nu_\tau) + BR(H^+ \to q\overline{q}') = 1$ is assumed, where $BR(H^+ \to q\overline{q}')$ is the sum of all hadronic branching ratios of the charged Higgs boson.

2 OPAL detector and Monte Carlo generation

The OPAL detector [13], with its acceptance of nearly 4π steradians, and its good tracking, calorimetry and particle identification capabilities, is well suited for this analysis which searches for widely different event topologies. The apparatus is composed of a central tracking detector, consisting of a silicon microvertex detector [14] and several concentric drift chambers inside a 0.435 Tesla magnetic field, surrounded by presamplers, time-of-flight scintillators and a lead-glass electromagnetic calorimeter located outside the magnet coil. The magnet return yoke is instrumented for hadron calorimetry and is covered by external muon chambers. Lead-scintillator detectors, the forward detector and gamma catcher, and silicon-tungsten calorimeters close to the beam axis complete the geometrical acceptance down to 25 mrad polar angle[1].

The signal selection efficiencies and the background contributions are estimated using Monte Carlo samples processed with a full simulation of the OPAL detector [15]. To generate the $e^+e^- \to H^+H^-$ events the PYTHIA [12] and HZHA [16] program packages are used. Both include initial and final state radiation. The generated partons are hadronized using JETSET [12]. Signal samples of 500 events for the $c\bar{s}s\bar{c}$, $\tau^+\nu_\tau s\bar{c}$ and $\tau^+\nu_\tau\tau^-\bar{\nu}_\tau$ final states are produced at fixed values of $M_{H^\pm}$ between 40 and 75 GeV in steps of 5 GeV. For systematic checks some high statistics samples of 2500 events are also generated with different quark flavors in the final state.

The background estimates from the different Standard Model processes are based on the following event generators: PYTHIA is used to generate $q\bar{q}(\gamma)$ processes, EXCALIBUR [17] and GRC4F [18] for four-fermion final states, BHWIDE [19] for $e^+e^-(\gamma)$, KORALZ [20] for $\mu^+\mu^-(\gamma)$ and $\tau^+\tau^-(\gamma)$, while PYTHIA, PHOJET [21], HERWIG [22] and VERMASEREN [23] for $e^+e^-q\bar{q}$ and $e^+e^-\ell^+\ell^-$ four-fermion final states from two-photon processes.

3 Event selection

The present search is performed at center-of-mass energies between 130 and 172 GeV, with integrated luminosities measured by the silicon-tungsten calorimeters of approximately 2.5 pb^{-1} at both 130 and 136 GeV, 10.0 pb^{-1} at 161 GeV and 10.3 pb^{-1} at 172 GeV with 0.5−1.4% error, depending on the center-of-mass energy, dominated by statistics. The analysis is sensitive to all dominant H^+H^- final states, namely, the hadronic $q\overline{q}'q''\overline{q}'''$, the semi-leptonic[2] $\tau^+\nu_\tau q\overline{q}'$ and the leptonic $\tau^+\nu_\tau\tau^-\bar{\nu}_\tau$ final states. The integrated luminosities can differ from channel to channel by less than 10%, since different detectors are required to be fully operational in the different analyses.

The event analysis uses charged particle tracks, electromagnetic and hadronic calorimeter clusters selected by a set of quality requirements similar to those used in previous Higgs boson

[1]The OPAL coordinate system is a right-handed 3-dimensional Cartesian coordinate system with its origin at the nominal interaction point, z-axis along the nominal electron beam direction and x-axis horizontal and directed towards the center of LEP. The polar angle, θ is defined with respect to the $+z$ direction and the azimuthal angle, ϕ with respect to the $+x$ direction.

[2]The charge-conjugate final state $q'\overline{q}\tau^-\bar{\nu}_\tau$ is also implied.

searches [24]. The quality requirements applied in the search for the leptonic final state are described in Reference [28]. Energy correction algorithms [25, 26] are used to prevent double counting in the case of charged tracks and associated calorimeter clusters.

3.1 The leptonic final state

A search for anomalous production of di-lepton events with missing transverse momentum has been presented in Reference [27] at $\sqrt{s}$ = 130−136 GeV and in Reference [28] at $\sqrt{s}$ = 161−172 GeV. The latter includes a search for pair-produced charged Higgs bosons in the leptonic channel, $H^+H^- \to \tau^+\nu_\tau\tau^-\bar{\nu}_\tau$. At $\sqrt{s}$ = 130−136 GeV the results of the search for pair-produced scalar tau leptons are used, since the experimental signature of $H^+H^- \to \tau^+\nu_\tau\tau^-\bar{\nu}_\tau$ is identical to that of scalar tau ($\tilde{\tau}^\pm$) pair-production, $\tilde{\tau}^+\tilde{\tau}^- \to \tau^+\tilde{\chi}^0_1\tau^-\tilde{\chi}^0_1$, for the case when the lightest neutralino, $\tilde{\chi}^0_1$, is massless and stable. The experimental methods and results of the analyses are summarized below. For details refer to [27, 28].

The signature for $H^+H^- \to \tau^+\nu_\tau\tau^-\bar{\nu}_\tau$ is a pair of tau leptons together with missing energy and momentum. Tau leptons may be identified by their decays into electrons, muons or hadrons. In selecting candidate events the missing momentum is required to have a significant component in the plane perpendicular to the beam axis and the total missing momentum vector must point away from the beam axis. Thereby Standard Model background with high energy particles escaping down the beam pipe and giving rise to missing momentum along the beam axis, is rejected.

A background that survives the above cuts arises from lepton pairs produced in two-photon processes in which one of the initial state electron is scattered at a significant angle to the beam direction. Events that may have arisen from such processes are suppressed by vetoing on energy being present in the forward detector, gamma catcher or silicon tungsten calorimeters.

To further suppress the remaining Standard Model background mainly from W^+W^- production and two-photon processes additional cuts on the momentum of the observed particles are applied. The cut values are optimized separately for each value of $M_{H^\pm}$ considered using an automated optimization procedure.

The results of the analysis are summarized in Table 1. Three candidates are selected in agreement with the Standard Model expectation. None of them have identified electrons or muons, so all tau lepton candidates are consistent with hadronic decays.

In addition to the uncertainty due to the limited Monte Carlo statistics a 5% systematic error is assigned to the estimated selection efficiency to take into account deficiencies in the Monte Carlo generators and the detector simulation.

The dominant background at $\sqrt{s}$ = 161−172 GeV results from W^+W^- production which is well understood and the available high statistics Monte Carlo samples describe well the OPAL data [29]. A 5% systematic error is assigned to the estimated background to take into account the uncertainty in the expected W^+W^- production cross-section arising from the uncertainty in the $W^\pm$ boson mass and deficiencies in the Monte Carlo detector simulation. At $\sqrt{s}$ = 130−136 GeV the dominant background comes from two-photon processes which are less

$\sqrt{s}$	$M_{\mathrm{H}^\pm}$ (GeV)							
(GeV)	40	45	50	55	60	65	70	75
Number of events selected								
133	0	0	0	0	0	0	–	–
161	1	1	1	1	1	1	1	–
172	2	2	2	2	2	2	2	2
Number of events expected from Standard Model processes								
133	1.1±0.4	1.1±0.4	1.1±0.4	1.1±0.4	1.1±0.4	1.1±0.4	–	–
161	0.9±0.2	0.8±0.1	1.0±0.2	1.1±0.2	1.1±0.2	1.1±0.2	1.0±0.2	–
172	1.0±0.1	1.2±0.2	1.3±0.2	1.4±0.2	1.4±0.2	1.4±0.2	1.4±0.2	1.5±0.2
Signal selection efficiency (%)								
133	27.6±1.5	31.1±1.5	34.6±1.5	37.6±1.5	38.2±1.5	40.2±1.6	–	–
161	44.2±2.2	46.8±2.2	50.2±2.2	51.2±2.2	53.0±2.2	56.4±2.2	59.0±2.2	–
172	29.0±2.0	35.0±2.1	40.4±2.2	44.6±2.2	46.2±2.2	46.6±2.2	51.2±2.2	50.8±2.2

Table 1: Leptonic Channel: The number of selected and expected events together with selection efficiencies at $\sqrt{s} = 130{-}136$, 161 and 172 GeV for different values of $M_{\mathrm{H}^\pm}$. The errors are statistical only. The dashes indicate masses which are kinematically forbidden or not simulated. Note that there is significant overlap between the various $M_{\mathrm{H}^\pm}$-dependent selections.

accurately modeled. The expected background at this center-of-mass energy is conservatively set to zero in the background subtraction procedure described in Section 4.

3.2 The semi-leptonic final state

The semi-leptonic channel $\mathrm{H}^+\mathrm{H}^- \to \tau^+\nu_\tau \mathrm{q}\overline{\mathrm{q}}'$ is characterized by an isolated tau lepton, a pair of acoplanar jets and sizeable missing momentum due to the undetected neutrinos. The selection is described below.

(1) The event must qualify as a hadronic final state as defined in [30].

(2) There must be at least one tau lepton identified following Reference [31], which has to be well isolated. The flight direction of the tau lepton is approximated by the direction of the momentum vector of its visible decay products. The ratio of both the track momenta ($R_{\mathrm{tr}}^{11/30}$) and the electromagnetic cluster energy ($R_{\mathrm{em}}^{11/30}$) within an 11° half-angle cone relative to that within a 30° half-angle cone around the direction of the tau lepton should be larger than 0.95 and the cosine of the angle between the direction of the tau lepton and the nearest track should be smaller than 0.94. If there is more than one tau lepton in the event and only one of them decays leptonically, that one is kept, otherwise the one with the largest $R_{\mathrm{tr}}^{11/30}$ is retained.

(3) Most of the two-photon and radiative two-fermion events are eliminated by requiring that the polar angle of the missing momentum, θ_p, satisfies $|\cos\theta_p| < 0.9$.

(4) Events with an energetic photon, identified as electromagnetic cluster with energy greater than 15 GeV that has no track within a 30° half-angle cone about the cluster axis, are rejected to eliminate the remaining radiative events.

(5) The two-fermion background is further reduced by requiring the visible invariant mass of the event, $M_{\rm vis} = \sqrt{E_{\rm vis}^2 - \vec{P}_{\rm vis}^2}$, to be smaller than $0.8\,\sqrt{s}$; the total missing momentum transverse to the beam direction, $p_{\rm T}$, to be larger than $0.13\,\sqrt{s}$ and the aplanarity[3] to exceed 0.005.

(6) At center-of-mass energies of 161−172 GeV to further suppress the remaining four-fermion background, mainly from $\rm W^+W^-$ with one $\rm W^\pm$ decaying leptonically, two additional conditions have to be satisfied. There should be no track in the event with momentum larger than $0.25\,\sqrt{s}$ and the cosine of jet-jet angle in the hadronic system must exceed -0.65 (-0.55) at $\sqrt{s} = 161$ (172) GeV. The two jets of the hadronic system obtained by removing the decay products of the tau lepton are defined using the Durham jet-finding algorithm [37].

Table 2 shows the number of selected data events, the total expected background and the signal efficiency for $M_{\rm H^\pm} = 50$ GeV after each cut at all four center-of-mass energies. The agreement between data and background simulation is good. After all requirements no event is selected in the data sample, while 2.7±0.2 (statistical error) events are expected from Standard Model processes. Of these, the four-fermion processes account for 13.3±3.0, 65.8±7.0 and 90.5±5.4% at $\sqrt{s} = 130-136$, 161 and 172 GeV, respectively.

In the semi-leptonic channel the Higgs mass can be reconstructed from the hadronic system with 2−3 GeV resolution by scaling the dijet invariant mass by the ratio of the beam energy to the total energy of the two jets. This simple correction improves the mass resolution by almost a factor of two and at the same time shifts the mass of the $\rm W^\pm$ bosons towards its nominal value, thereby decreasing the expected background in the mass range below 65 GeV. The mass distributions are shown in Figure 1 before and after cut (6) for the selected events and the expected background together with a signal of $M_{\rm H^\pm} = 50$ GeV. Note that cut (6) is also effective to reduce the background in the mass range below 60 GeV and that the remaining background is concentrated around a mass of 70 GeV.

The flavor independence of the selection is tested using Monte Carlo samples of $\rm H^+H^- \to \tau^+\nu_\tau s\bar{c}$ and $\rm H^+H^- \to \tau^+\nu_\tau b\bar{c}$. The observed differences are consistent within the statistical error of 2.4%, which is conservatively incorporated into the systematic error.

The signal selection efficiencies are affected by the following uncertainties: Monte Carlo statistics, see Table 3; uncertainties on the tau lepton identification efficiency (including the errors on electron and muon identification), 3%; modeling of the cut variables excluding the tau lepton identification, 6%; and dependence on the flavor of the final state quarks, 2.4%.

[3] Aplanarity is defined as $\frac{3}{2}\lambda_3$, where λ_i are the eigenvalues [$\lambda_1 \geq \lambda_2 \geq \lambda_3$ with $\lambda_1 + \lambda_2 + \lambda_3 = 1$] of the sphericity tensor $S^{\alpha\beta} = \sum_i p_i^\alpha p_i^\beta / \sum_i |\mathbf{p}_i|^2$, and measures the transverse momentum component out of the event plane.

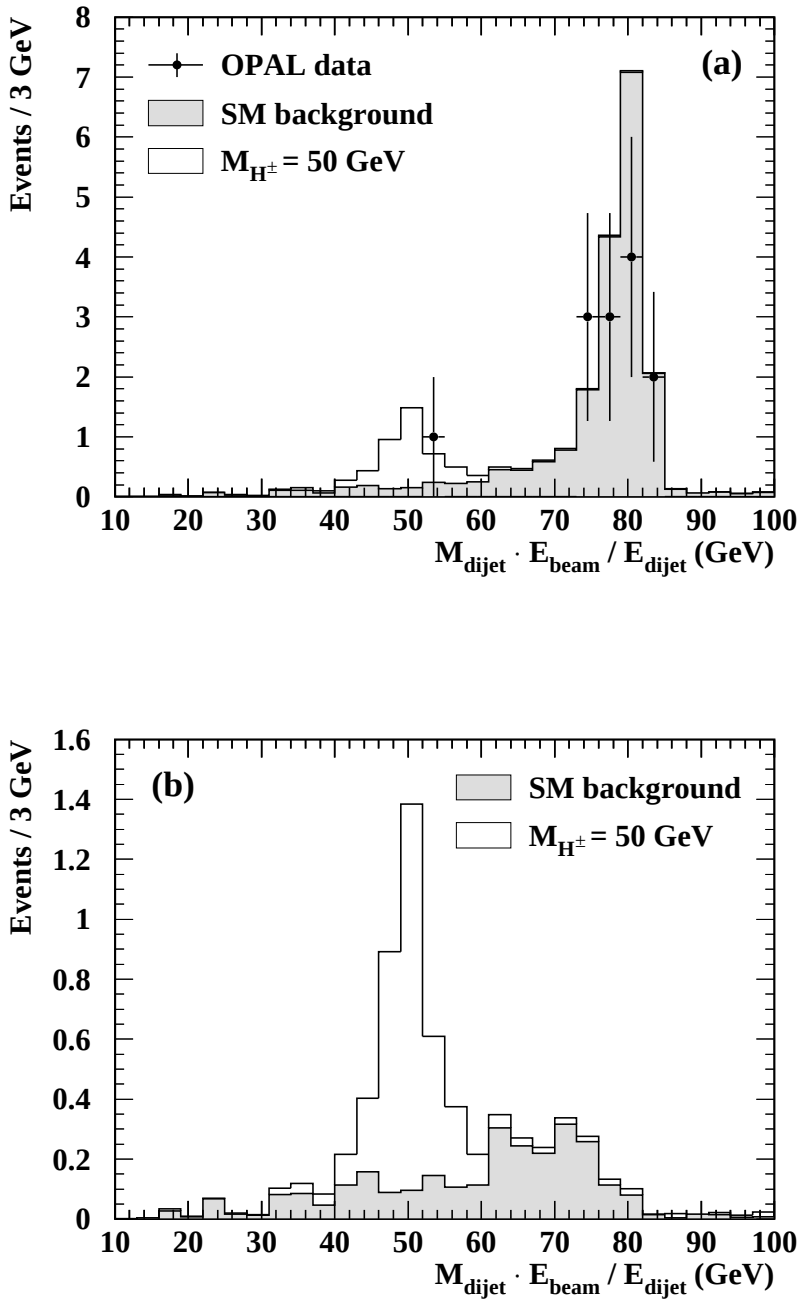

Figure 1: Semi-leptonic channel: Scaled invariant mass distributions at $\sqrt{s} = 130{-}172$ GeV normalized to the collected luminosity, (a) before cut (6) and (b) after all cuts. The selected events are shown as dots with error bars, the Standard Model background estimate as a shaded histogram and a signal sample for $M_{\mathrm{H}^\pm} = 50$ GeV assuming $\mathrm{BR}(\mathrm{H}^+ \to \tau^+\nu_\tau) = 0.5$ as an open histogram.

Cut	130 GeV			136 GeV		
	data	SM bgrd.	Efficiency [%]	data	SM bgrd.	Efficiency [%]
1	736	728.8±3.2	99.0±0.4	688	689.0±3.2	97.8±0.7
2	53	51.3±1.3	61.0±2.2	56	47.2±1.3	57.2±2.2
3	28	25.0±0.8	57.8±2.2	25	22.4±0.7	54.8±2.2
4	26	21.5±0.7	57.4±2.2	24	19.0±0.7	54.8±2.2
5	0	0.5±0.1	40.4±2.2	0	0.2±0.1	42.4±2.2
Cut	161 GeV			172 GeV		
	data	SM bgrd.	Efficiency [%]	data	SM bgrd.	Efficiency [%]
1	1509	1464.5±3.1	98.6±0.5	1394	1294.6±2.2	98.2±0.6
2	126	110.6±1.4	67.4±2.1	131	116.3±1.1	67.6±2.1
3	46	48.8±0.7	65.2±2.1	63	64.4±0.7	65.8±2.1
4	41	42.9±0.7	64.8±2.1	58	59.8±0.6	64.8±2.1
5	2	4.1±0.1	50.2±2.2	12	15.4±0.2	44.8±2.2
6	0	0.7±0.1	48.2±2.2	0	1.3±0.1	44.2±2.2

Table 2: Semi-leptonic channel: Comparison of the number of observed events and expected background together with the selected fraction of simulated signal events ($M_{\mathrm{H}^\pm} = 50$ GeV) after each cut. The errors are statistical only.

The background estimate has the following errors: Monte Carlo statistics, see Table 2; modeling of the hadronization process estimated by comparing different event generators, 9%; modeling of the variables used to identify tau leptons, 5%; and modeling of the remaining selection variables, 5%.

$\sqrt{s}$	Signal selection efficiencies (%) for $M_{\mathrm{H}^\pm}$							
(GeV)	40 GeV	45 GeV	50 GeV	55 GeV	60 GeV	65 GeV	70 GeV	75 GeV
130	37.0±2.2	42.4±2.2	40.4±2.2	35.0±2.1	27.6±2.0	–	–	–
136	37.0±2.2	45.6±2.2	42.4±2.2	38.6±2.2	35.0±2.1	–	–	–
161	42.6±2.2	46.0±2.2	48.2±2.2	43.0±2.2	35.0±2.1	31.0±2.1	26.8±2.0	–
172	41.8±2.2	43.2±2.2	44.2±2.2	42.2±2.2	37.0±2.2	35.8±2.1	29.8±2.0	12.2±1.5

Table 3: Semi-leptonic channel: Signal selection efficiencies for the various center-of-mass energies and charged Higgs masses. The errors are statistical only. The dashes indicate masses which are kinematically forbidden or not simulated. For higher masses the selection efficiency drops due to cut (6).

3.3 The hadronic final state

The hadronic channel, $H^+H^- \to q\overline{q}'q''\overline{q}'''$, is characterized by an event topology with four well separated hadron jets and large visible energy. The selection is described below.

(1) The event must qualify as hadronic final state as defined in [30].

(2) Events with a radiative photon or large missing energy are eliminated by requiring the effective center-of-mass energy, $\sqrt{s'}$, calculated as described in Reference [36], to be at least $0.87\sqrt{s}$ and the visible invariant mass to be at least $0.7\sqrt{s}$.

(3) The events are reconstructed into four jets using the Durham jet-finding algorithm [37] with the visible energy as the scale parameter. The jet resolution parameter, y_{34}, at which the number of jets changes from 3 to 4, has to be larger than 0.01 at $\sqrt{s} = 130{-}136$ GeV, and larger than 0.005 at $\sqrt{s} = 161{-}172$ GeV. The tighter cut at lower energies is necessary because of the higher $q\bar{q}$ background. Moreover each jet must contain at least one charged track.

(4) At $\sqrt{s} = 161{-}172$ GeV, the remaining radiative $q\bar{q}\gamma$ events are further suppressed by vetoing on jets with properties compatible with those of a radiative photon, namely, exactly one electromagnetic cluster, not more than two tracks and jet energy above $\sqrt{s} - 121$ GeV.

(5) To further reduce the $q\bar{q}$ background the following requirements are imposed: the polar angle of the thrust axis has to satisfy $|\cos\theta_{\rm thr}| < 0.8$; the event shape parameter[4], C, has to be larger than 0.6 at $\sqrt{s} = 130{-}136$ GeV and larger than 0.45 at $\sqrt{s} = 161{-}172$ GeV; and the cosine of the angle between any pair of jets must be smaller than 0.62 at $\sqrt{s} = 130{-}136$ GeV and 0.66 at higher center-of-mass energies.

(6) To test the compatibility of the event with the decay of two equal mass objects a four-constraint kinematic fit requiring energy and momentum conservation is performed and the mass difference between the two dijet systems is calculated for all three possible jet pair combinations. The event is discarded if the χ^2-probability of the fit is below 0.01 or if the smallest mass difference is larger than 6 GeV at $\sqrt{s} = 130{-}136$ GeV and 8 GeV at higher center-of-mass energies. For all events passing this cut, to obtain the best possible dijet mass resolution a five-constraint kinematic fit is performed for all three jet pair combinations imposing energy and momentum conservation and equal dijet invariant masses and the event is rejected if the largest χ^2-probability is below 0.01.

(7) At center-of-mass energies of 161 GeV and above a veto is applied against W^+W^- events using the dijet masses calculated after the four-constraint kinematic fit. At $\sqrt{s} = 161$ GeV, since the $W^\pm$ bosons are produced practically at rest, the two jets having the largest measured opening angle are assigned to one of the $W^\pm$ bosons and the two remaining jets to the other. An event is rejected if both jet pairs have an invariant mass greater

[4] The C parameter is defined as $C = (\lambda_1\lambda_2 + \lambda_1\lambda_3 + \lambda_2\lambda_3)$, where λ_i are the eigenvalues $[\lambda_1 + \lambda_2 + \lambda_3 = 1]$ of the generalized sphericity tensor $S^{(1)\alpha\beta} = \sum_i (p_i^\alpha p_i^\beta/|\mathbf{p}_i|)/\sum_i |\mathbf{p}_i|$.

than 70 GeV. At $\sqrt{s} = 172$ GeV the event is rejected if any of the three possible jet pair combinations yields invariant masses greater than 74 GeV for both of the two dijet systems.

For the remaining events, the jet pair association giving the highest χ^2-probability in the five-constraint kinematic fit is retained. The resulting mass resolution is 1.0−1.5 GeV.

Table 4 shows the number of selected events, the estimated background and the fraction of signal events retained for $M_{\mathrm{H}^\pm} = 50$ GeV at all center-of-mass energies after each cut. The agreement between data and expected background is good. In total, twelve events are selected in the data, while 15.3±0.4 (statistical error) events are expected from Standard Model processes. The four-fermion processes account for 10.1±1.2, 32.3±1.7 and 64.8±3.5% of the expected background at $\sqrt{s} = 130-136$, 161 and 172 GeV, respectively. Figure 2 shows the invariant mass distribution of the selected events together with the Standard Model background expectation and a signal of $M_{\mathrm{H}^\pm} = 50$ GeV.

	130 GeV			136 GeV		
Cut	data	SM bgrd.	Efficiency [%]	data	SM bgrd.	Efficiency [%]
1	744	733.8±3.2	99.8±0.2	676	679.7±3.1	99.8±0.2
2	173	201.7±2.1	94.2±1.0	184	180.2±1.9	93.0±1.1
3	11	11.5±0.6	62.8±2.2	14	11.6±0.6	59.4±2.2
5	4	3.7±0.3	49.2±2.2	4	3.9±0.3	50.4±2.2
6	2	1.2±0.2	33.4±2.1	2	1.6±0.2	34.4±2.1
	161 GeV			172 GeV		
Cut	data	SM bgrd.	Efficiency [%]	data	SM bgrd.	Efficiency [%]
1	1497	1453.5±3.1	100.0±0.2	1393	1310.8±3.4	100.0±0.2
2	392	374.5±1.4	93.6±1.1	359	368.9±1.3	94.6±1.0
3	62	53.2±0.5	75.6±1.9	88	82.5±0.5	72.2±2.0
4	59	50.8±0.5	75.6±1.9	87	80.2±0.5	72.2±2.0
5	21	19.2±0.3	67.2±2.1	36	38.1±0.3	59.4±2.2
6	8	8.9±0.2	52.4±2.2	14	18.6±0.3	48.8±2.2
7	3	5.0±0.2	45.4±2.2	5	7.5±0.2	42.2±2.2

Table 4: Hadronic channel: Comparison of the number of observed events and expected background together with the selected fraction of simulated signal events ($M_{\mathrm{H}^\pm} = 50$ GeV) after each cut. The errors are statistical only.

The systematic effects on the signal selection efficiency are the following: Monte Carlo statistics, see Table 5; final-state quark flavor dependence, 2.4%; and modeling of the cut variables, 5%.

The background estimate is affected by the following systematic uncertainties: limited Monte Carlo statistics, see Table 4; modeling of the hadronization process estimated by comparing different event generators, 7%; modeling of the cut variables, 6%. Since the theoretical uncertainty on the prediction of the QCD four-jet rates is not known, conservatively its experimental error of 15% [38] is taken which is dominated by statistics. Taking into account the relative weight of the QCD background, this results in an 8% error on the background estimate.

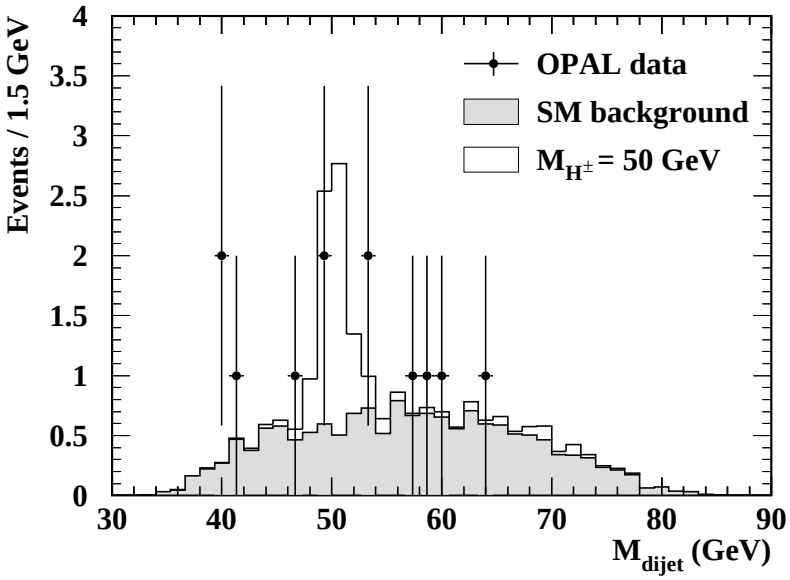

Figure 2: Hadronic channel: Invariant mass distribution using a five-constraint kinematic fit at $\sqrt{s} = 130{-}172$ GeV normalized to the collected luminosity, after all cuts. The selected events are shown as dots with error bars, the Standard Model background estimate as a shaded histogram and a signal sample for $M_{\mathrm{H}^\pm} = 50$ GeV assuming $\mathrm{BR}(\mathrm{H}^+ \to \mathrm{q}\overline{\mathrm{q}}') = 1$ as an open histogram.

$\sqrt{s}$	Signal selection efficiencies (%) for $M_{\mathrm{H}^\pm}$							
(GeV)	40 GeV	45 GeV	50 GeV	55 GeV	60 GeV	65 GeV	70 GeV	75 GeV
130	32.4±2.1	32.4±2.1	33.4±2.1	29.6±2.0	22.2±1.9	–	–	–
136	29.8±2.0	36.6±2.2	34.6±2.1	26.0±2.0	26.8±2.0	–	–	–
161	36.0±2.1	41.4±2.2	45.4±2.2	41.4±2.2	36.4±2.2	31.4±2.1	28.0±2.0	–
172	24.6±1.9	40.4±2.2	42.2±2.2	39.6±2.2	39.0±2.2	29.4±2.0	31.2±2.1	20.0±1.8

Table 5: Hadronic channel: Signal selection efficiencies for the various center-of-mass energies and charged Higgs masses. The errors are statistical only. The dashes indicate masses which are kinematically forbidden or not simulated. For higher masses the detection efficiency drops due to cut (7).

4 Results

The statistical method of Reference [39] is used to calculate 95% confidence level lower limits on the charged Higgs boson mass. This method has been developed to derive exclusion limits for particle searches when several candidate events are observed in different decay channels with different mass resolutions and different background conditions. The method introduces an event weight for each channel and derives the confidence limit from the sum of the event weights for all candidates. The mass spectrum of the background is also taken into account.

The predicted background is accounted for by considering the selected events as *signal plus background*. In the calculation of the limit the expected background is decreased by its statistical and systematic error.

The lower bounds on the mass of the charged Higgs boson, at the 95% confidence level, obtained from the searches in the leptonic, semi-leptonic and hadronic channels, are presented in Figure 3 as a function of the $H^+ \to \tau^+\nu_\tau$ branching ratio. The limits are obtained using the cross section calculated by PYTHIA for the process $e^+e^- \to H^+H^-$. They take into account the integrated luminosities of the data and the selection efficiencies as a function of $M_{H^\pm}$ at each center-of-mass energy. The uncertainty on the signal efficiency is incorporated into the limit using the method described in Reference [40].

Charged Higgs bosons are excluded at 95% confidence level independent of the $H^+ \to \tau^+\nu_\tau$ branching ratio up to a mass of 52 GeV. Upper limits on the production cross-section times branching fraction of the decay to a given final state assuming the s-dependence of the charged Higgs boson production cross-section, scaled to $\sqrt{s} = 172$ GeV, are presented in Figure 3 for all three final states.

Acknowledgements

We particularly wish to thank the SL Division for the efficient operation of the LEP accelerator at all energies and for their continuing close cooperation with our experimental group. We thank our colleagues from CEA, DAPNIA/SPP, CE-Saclay for their efforts over the years on the time-of-flight and trigger systems which we continue to use. In addition to the support staff at our own institutions we are pleased to acknowledge the
Department of Energy, USA,
National Science Foundation, USA,
Particle Physics and Astronomy Research Council, UK,
Natural Sciences and Engineering Research Council, Canada,
Israel Science Foundation, administered by the Israel Academy of Science and Humanities,
Minerva Gesellschaft,
Benoziyo Center for High Energy Physics,
Japanese Ministry of Education, Science and Culture (the Monbusho) and a grant under the Monbusho International Science Research Program,
German Israeli Bi-national Science Foundation (GIF),
Bundesministerium für Bildung, Wissenschaft, Forschung und Technologie, Germany,

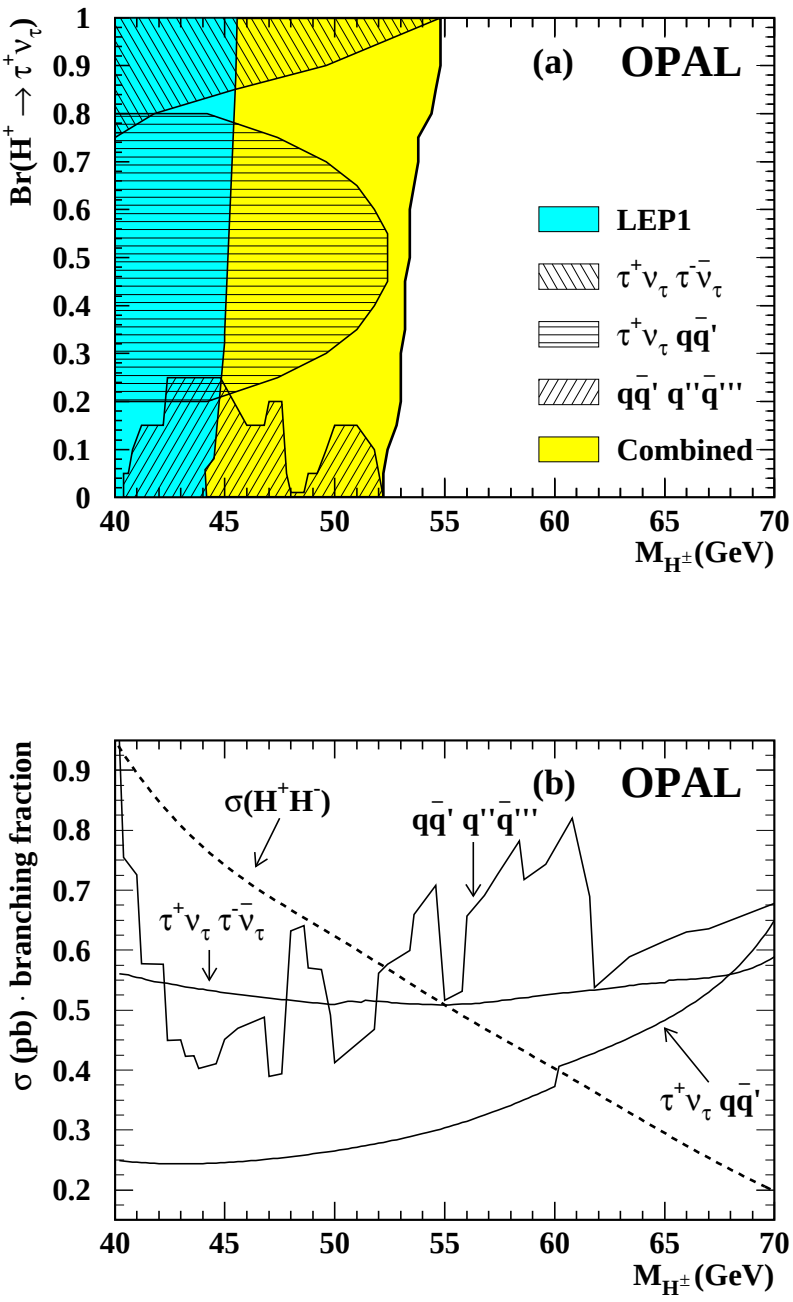

Figure 3: (a) Excluded areas at 95% confidence level in the [$M_{\mathrm{H}^\pm}$, BR($\mathrm{H}^+ \to \tau^+\nu_\tau$)] plane. The dark shaded area is excluded by LEP1 and the light shaded area by the present search. The results from each of the channels separately are indicated by different hatch styles. (b) Upper limits, scaled to $\sqrt{s} = 172$ GeV, on the production cross-section times branching fraction of the decay to a given final state, at 95% confidence level, calculated using the s-dependence of the charged Higgs boson production cross-section for each channel. The charged Higgs boson production cross-section at $\sqrt{s} = 172$ GeV is also shown as a dashed line. Note that the maximum branching fraction for the $\tau^+\nu_\tau \mathrm{q}\overline{\mathrm{q}}'$ final state is 0.5.

National Research Council of Canada,
Research Corporation, USA,
Hungarian Foundation for Scientific Research, OTKA T-016660, T-023793 and OTKA F-023259.

References

[1] S. Weinberg, *Phys. Rev. Lett.* **19** (1967) 1264;
A. Salam, in *Elementary Particle Theory*, edited by N. Svartholm (Almqvist and Wiksell, Stockholm, 1968), p. 367;
S. L. Glashow, *Nucl. Phys.* **B22** (1961) 579;
S. L. Glashow, J. Iliopoulos and L. Maiani, *Phys. Rev.* **D2** (1970) 1285.

[2] P. W. Higgs, *Phys. Lett.* **12** (1964) 132;
F. Englert and R. Brout, *Phys. Rev. Lett.* **13** (1964) 321; *Phys. Rev.* **145** (1966) 1156;
G. S. Guralnik, C. R. Hagen and T. W. Kibble, *Phys. Rev. Lett.* **13** (1964) 585.

[3] See, e.g., J. F. Gunion, H. E. Haber, G. L. Kane and S. Dawson, *The Higgs Hunter's Guide* (Addison-Wesley, 1990).

[4] Y. Gol'fand, E. Likhtam, *JETP Lett.* **13** (197) 323;
D. Volkov, V. Akulov, *Phys. Lett.* **B46** (1973) 109;
J. Wess, B. Zumino, *Nucl. Phys.* **B70** (1974) 39.

[5] M. Carena, J. R. Espinosa, M. Quirós, C. E. M. Wagner, *Phys. Lett.* **B355** (1995) 209.

[6] OPAL Collaboration, G. Alexander et al., *Phys. Lett.* **B370** (1996) 74;
DELPHI Collaboration, P. Abreu et al., *Z. Phys.* **C64** (1994) 183;
ALEPH Collaboration, D. Decamp et al., *Phys. Rep.* **V216** (1992) 253;
L3 Collaboration, O. Adriani et al., *Phys. Lett.* **B294** (1992) 457.

[7] DELPHI Collaboration, P. Abreu et al., *Search for charged Higgs bosons in e^+e^- collisions at $\sqrt{s}$ = 172 GeV*, CERN-PPE/97-145, subm. to *Phys. Lett.* **B**;
ALEPH Collaboration, R. Barate et al., *Search for charged Higgs bosons in e^+e^- collisions at center-of-mass energies from 130 to 172 GeV*, CERN-PPE/97-129, subm. to *Phys. Lett.* **B**.

[8] CLEO Collaboration, M. S. Alam et al., *Phys. Rev. Lett.* **74** (1995) 2885.

[9] T. Goto, Y. Okada, *Progr. Theor. Phys. Suppl.* **123** (1996) 213.

[10] CDF Collaboration, F. Abe et al., *Phys. Rev. Lett.* **79** (1997) 357.

[11] A. Djouadi, J. Kalinowski, P. M. Zerwas, *Z. Phys.* **C57** (1993) 569.

[12] PYTHIA 5.721 and JETSET 7.408 generators: T. Sjöstrand, *Comp. Phys. Comm.* **82** (1994) 74; LU TP 95-20 and CERN-TH.7112/93 (revised August 1995).

[13] OPAL Collaboration, K. Ahmet et al., *Nucl. Instrum. Methods* **A305** (1991) 275.

[14] P. P. Allport et al., *Nucl. Instrum. Methods* **A324** (1993) 34; P. P. Allport et al., *Nucl. Instrum. Methods* **A346** (1994) 476.

[15] J. Allison et al., *Nucl. Instrum. Methods* **A317** (1992) 47.

[16] HZHA generator: G. Ganis and P. Janot, in *Physics at LEP2*, edited by G. Altarelli, T. Sjöstrand and F. Zwirner, CERN 96-01, Vol. 2 (1996), p. 299.

[17] EXCALIBUR generator: F. A. Berends, R. Pittau, R. Kleiss, *Comp. Phys. Comm.* **85** (1995) 437.

[18] GRC4F 1.1 generator: J. Fujimoto et al., *Comp. Phys. Comm.* **100** (1997) 128.

[19] BHWIDE generator: S. Jadach, W. Placzek, B. F. L. Ward *Phys. Lett.* **B 390** (1997) 298.

[20] KORALZ 4.0 generator: S. Jadach, B. F. L. Ward, Z. Wąs, *Comp. Phys. Comm.* **79** (1994) 503.

[21] PHOJET generator: R. Engel and J. Ranft, *Phys. Rev.* **D54** (1996) 4244.

[22] HERWIG 5.9 generator: G. Marchesini et al., *Comp. Phys. Comm.* **67** (1992) 465.

[23] VERMASEREN generator: J. A. M. Vermaseren, *Nucl. Phys.* **B229** (1983) 347.

[24] OPAL Collaboration, R. Akers et al., *Phys. Lett.* **B327** (1994) 397.

[25] OPAL Collaboration, M. Z. Akrawy et al., *Phys. Lett.* **B253** (1991) 511.

[26] OPAL Collaboration, K. Ackerstaff et al., *Phys. Lett.* **B389** (1996) 616.

[27] OPAL Collaboration, G. Alexander et al., *Z. Phys.* **C73** (1997) 201.

[28] OPAL Collaboration, K. Ackerstaff et al., *Search for anomalous production of di-lepton events with missing transverse momentum in e^+e^- collisions at $\sqrt{s}$ = 161 and 172 GeV*, CERN-PPE/97-124, subm. to *Z. Phys* **C**.

[29] OPAL Collaboration, K. Ackerstaff et al., *Measurement of the W boson mass and W^+W^- production and decay properties in e^+e^- collisions at $\sqrt{s}$ = 172 GeV*, CERN-PPE/97-116, subm. to *Z. Phys* **C**;
OPAL Collaboration, K. Ackerstaff et al., *Phys. Lett.* **B389** (1996) 416.

[30] OPAL Collaboration, G. Alexander et al., *Z. Phys.* **C52** (1991) 175.

[31] OPAL Collaboration, K. Ackerstaff et al., *Phys. Lett.* **B393** (1996) 231;
OPAL Collaboration, K. Ackerstaff et al., *Search for the Standard Model Higgs boson in e^+e^- collisions at $\sqrt{s}$ = 161−172 GeV*, CERN-PPE/97-115, accepted by *Z. Phys.* **C**.

[32] OPAL Collaboration, R. Akers et al., *Phys. Lett.* **B327** (1994) 411.

[33] OPAL Collaboration, G. Alexander et al., *Z. Phys.* **C70** (1996) 357.

[34] OPAL Collaboration, G. Alexander et al., *Z. Phys.* **C52** (1991) 175.

[35] OPAL Collaboration, R. Akers et al., *Z. Phys.* **C63** (1994) 197.

[36] OPAL Collaboration, G. Alexander et al., *Phys. Lett.* **B376** (1996) 232.

[37] S. Catani, Yu. L. Dokshitzer, M. Olsson, G. Turnock and B. R. Webber, *Phys. Lett.* **B269** (1991) 432.

[38] The OPAL Collaboration, K. Ackerstaff et al., *Z. Phys.* **C75** (1997) 193.

[39] P. Bock, *Determination of exclusion limits for particle production using different decay channels with different efficiencies, mass resolutions and backgrounds*, Heidelberg University preprint HD-PY-96/05 (1996).

[40] R. D. Cousins and V. L. Highland, *Nucl. Instrum. Methods* **A320** (1992) 331.